Fast ion diffusion, superionic conductivity and phase transitions of the nuclear materials UO_2 and Li_2O

2007 J. Phys.: Condens. Matter 19 386239

(http://iopscience.iop.org/0953-8984/19/38/386239)

J. Phys.: Condens. Matter **19** (2007) 386239 (8pp) doi:10.1088/0953-8984/19/38/386239

Fast ion diffusion, superionic conductivity and phase transitions of the nuclear materials UO_2 and Li_2O

Prabhatasree Goel, N Choudhury and S L Chaplot

Solid State Physics Division, Bhabha Atomic Research Centre, Mumbai 400 085, India

Received 29 June 2007, in final form 20 July 2007
Published 6 September 2007
Online at stacks.iop.org/JPhysCM/19/386239

Abstract
Lattice dynamics and molecular dynamics studies of the oxides UO_2 and Li_2O in their normal as well as superionic phases are reported. Lattice dynamics calculations have been carried out using a shell model in the quasiharmonic approximation. The calculated elastic constants, phonon frequencies and specific heat are in good agreement with reported experimental data, which help validate the interatomic potentials required for undertaking molecular dynamics simulations. The calculated free energies reveal high pressure fluorite to cotunnite phase transitions at 70 GPa for UO_2 and an anti-fluorite to anti-cotunnite phase transformation at 25 GPa for Li_2O, in agreement with reported experiments. Molecular dynamics studies provide important insights into the mechanisms of diffusion and superionic behaviour at high temperatures. The calculated superionic transition temperature of Li_2O is 1000 K, while that of UO_2 is 2300 K.

1. Introduction

UO_2 is of technological importance owing to its use as a nuclear fuel [1]. Knowledge of the thermodynamic and transport properties of nuclear materials [1–18] at high temperatures is of great interest. UO_2 belongs to the class of superionics wherein fast ion conduction processes involving rapid diffusion of a significant fraction of the oxygen atoms within an essentially rigid framework of uranium atoms occurs. Microscopic modelling or simulation is necessary to understand the conduction processes and thermodynamic properties at high temperatures and pressures of superionic crystals. UO_2 has a face-centred-cubic fluorite structure having space group O_h^5 ($Fm3m$), with the oxygen atoms in the tetrahedral sites. UO_2 and Li_2O show a type II superionic transition [1, 10] attaining high levels of ionic conductivity following a gradual and continuous disordering process within the same phase.

Several theoretical and experimental works [4, 19–30] have been reported on numerous fast ion conductors like Li_2O, CaF_2, BaF_2, PbF_2, $SrCl_2$, CuI, etc. The main impetus for these studies has been a desire to unravel the causes behind the process of fast ion conduction. In the case of Li_2O, there has been further interest in studying Li diffusion from the point of view of tritium generation for future fusion reactors. The oxides Li_2O and UO_2 behave similarly to other superionic halides. The extensive diffusion is characterized by a large decrease in the elastic constant C_{11} and specific heat anomaly at the transition temperature T_c [28–33]. Neutron scattering measurements [34] indicate that the anionic sublattice in UO_2 becomes heavily disordered in the region of 2300 K. Measured elastic constants [35] do show a softening above 2400 K in the region where fast ion behaviour is expected in UO_2, but the variation below this temperature is already very large. There is a large increase in specific heat [36–38] at high temperatures in UO_2. Li_2O shows a sudden decrease in the value of the C_{11} elastic constant at the transition temperature, $T_c \sim 1200$ K (the melting point T_m of Li_2O is 1705 K [22]), but there seems no drastic change in the specific heat [39, 40]. Both these compounds conform with the general belief that fluorites (anti-fluorites) in general show a diffuse transition at about $0.8T_m$ (T_m = melting point; T_m for UO_2 is 3120 K). Above the transition temperature the diffusion coefficient of one of the constituent atoms becomes comparable to that of liquids. Detailed study of the processes occurring in the crystal lattice at elevated temperatures is essential to understand the transitions.

Angle dispersive synchrotron x-ray powder diffraction and Raman spectroscopy experiments reveal a reversible phase transition from cubic anti-fluorite to the orthorhombic anti-cotunnite structure at a pressure near 50 GPa for Li_2O [41–43]. This transition is accompanied by a relatively large volume collapse of about $5.4(\pm 0.8)\%$ and a large hysteresis upon pressure reversal (P_{down} at $\sim$25 GPa). Similarly, UO_2 also shows a sluggish transformation to the cotunnite-type phase at about 40 GPa; the cotunnite phase coexists with the fluorite phase even at 69 GPa [44, 45].

The present study is aimed at formulating a suitable interatomic potential for explaining the vibrational properties of the oxides in concurrence with the available experimental data, as in our previous work [4]. The main objectives of the present study are: (i) to determine a suitable interatomic potential model for calculating the phonon spectrum, specific heat, other thermodynamic and elastic properties, (ii) to carry out molecular dynamics simulations using these interatomic potentials to elucidate diffusion behaviour and the thermodynamic properties of the oxides at elevated temperatures, and (iii) to study the phase transformation from the fluorite (anti-fluorite) to the cotunnite (anti-cotunnite) phase.

2. Lattice dynamics calculations and molecular dynamics calculations

Our calculations have been carried out in the quasiharmonic [46–49] approximation using the interatomic potentials consisting of Coulomb and short-range Born–Mayer type interaction terms:

$$V(r_{ij}) = \frac{e^2}{4\pi\varepsilon_0}\frac{Z(k)Z(k')}{r_{ij}^2} + a\exp\left[\frac{-br_{ij}}{R(k)+R(k')}\right] \tag{1}$$

where r_{ij} is the separation between the atoms i and j of type k and k' respectively. $R(k)$ and $Z(k)$ are the effective radius and charge of the kth atom, $a = 1822$ eV and $b = 12.364$ are the empirical parameters optimized from several previous calculations [48, 49]. The optimized parameters used in Li_2O are as given in [4]. In the case of UO_2, $Z[O] = -1.45$, $Z[U] = 2.9$, $R[O] = 0.175$ nm and $R[U] = 0.21$ nm, respectively. Oxygen atoms have been modelled using a shell model [46, 47], where a massless shell of charge $Y(k)$ (in UO_2, $Y(O) = -2$) is linked to the atomic core by the harmonic force constant $K(k)$ ($K(O)$ in UO_2 is 11 000 eV nm^{-2}). The lattice constant, zone centre phonon frequencies and elastic constants have been fitted to experimental values. The calculations have been carried out using the current version of the software DISPR developed in Trombay [50, 51]. The interatomic potential enables the

Table 1. Comparison between the calculated and experimental lattice parameters, elastic constants of Li_2O and UO_2.

Physical quantity	Calc. Li_2O	Expt. Li_2O [2, 39]	Calc. UO_2	Expt. UO_2 [34]
Lattice parameter (nm)	0.461	0.46	0.546	0.547
Bulk modulus (GPa)	103	82	180.5	207
C_{11} (GPa)	213	202	387	389
C_{44} (GPa)	52	59	66	60
C_{12} (GPa)	56	21	77	119

calculation of the phonon frequencies for the entire Brillouin zone. On the basis of the crystal symmetry, group theoretical analysis provides a classification of the frequencies at zone centre and the symmetry directions, in the various representations.

Molecular dynamics provides a powerful method for exploring the structure and dynamics of solids, liquids and gases. Explicit computer simulation of the structure and dynamics using this technique allows a microscopic insight into the behaviour of materials for understanding the macroscopic phenomena like diffusion of lithium (oxygen in the case of UO_2) ions and their contribution to the fast ion transition in this case. An interatomic potential which treats Li, U and O as rigid units may be sufficient for studying properties like diffusion. The optimized parameters obtained from lattice dynamics studies have been used for these simulations. In our study, we have taken a macrocell of a large number of rigid atoms with periodic boundary conditions to study the response of the system when set free to evolve from a configuration disturbed from the equilibrium situation. The lattice parameters and atomic trajectories can thus be obtained as a function of temperature and external pressure. Calculations in this work have been done using the software developed at Trombay [51–54]. The simulations have been done at various temperatures up to and beyond the fast ion transition. In our study we have considered a macrocell of 768 rigid atoms with periodic boundary conditions in the case of Li_2O and 1500 rigid atoms in the case of UO_2.

3. Results and discussion

3.1. Phonon spectra and elastic properties

The calculated values of the lattice parameter, bulk modulus, and elastic constants compare well with the experimentally obtained data as given in table 1. Figure 1 gives the computed phonon dispersion relations in Li_2O [4] and UO_2 along the various high symmetry directions, which are in good agreement with available experimental data [55, 56]. The elastic behaviour of the two oxides is markedly different (table 1). UO_2 is a harder material with almost twice the bulk modulus value as compared to Li_2O.

The total and partial densities of Li_2O [4] and UO_2 are given in figure 2. In the case of Li_2O, the energy spans the spectral range up to 90 meV, while for UO_2 it is up to 75 meV. From the partial densities of states, we conclude that Li atoms in Li_2O contribute almost over the entire range up to 75 meV with a significant contribution at 90 meV as well. Uranium's contribution is restricted to up to 25 meV only. The diffusing atom [57] Li in Li_2O shows a behaviour similar to the one exhibited by oxygen in UO_2, but owing to its large mass, uranium's behaviour is clearly opposite to that of the non-diffusing oxygen in Li_2O. The oxygens contribute over the entire energy range, although their spectra are different in Li_2O and UO_2.

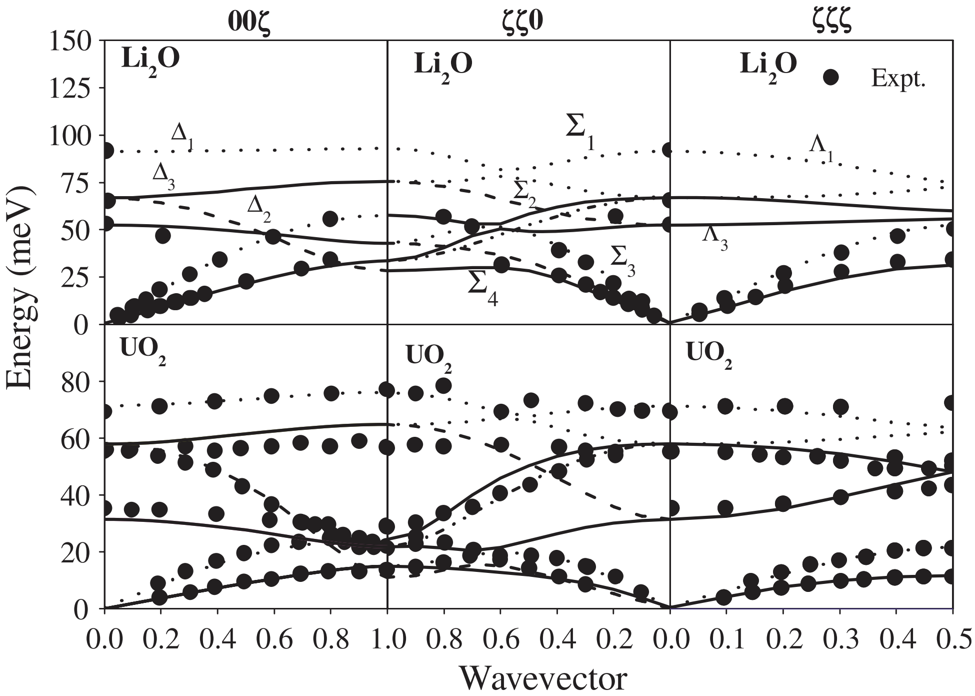

Figure 1. Comparison of the calculated (full, dashed and dash–dot lines) phonon dispersion relations with experimental (symbols) neutron scattering data for Li_2O [55] and UO_2 [56].

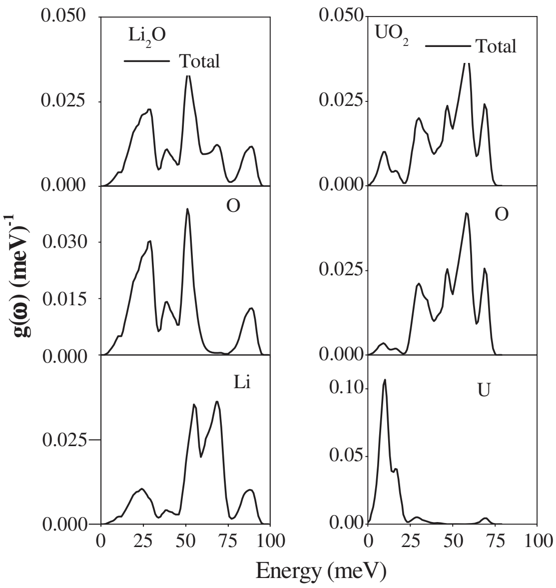

Figure 2. Phonon density of states along with the partial density of states for lithium, oxygen and uranium for Li_2O and UO_2 as calculated by quasiharmonic lattice dynamics calculations.

3.2. Specific heat

The calculated density of states has been used to evaluate various thermodynamic properties of the two oxides. Calculated specific heats at constant pressure, $C_P(T)$, have been compared with

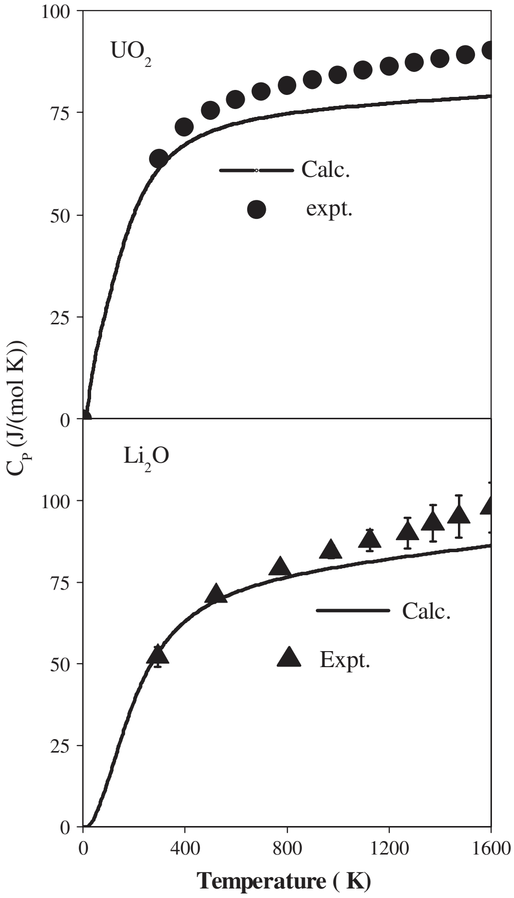

Figure 3. Specific heat at constant pressure compared with experimental data (closed symbols) for UO_2 [36] and Li_2O [39].

Table 2. Comparison of the calculated Frenkel defect energies E_F (eV) with reported first-principles [14, 33] and atomistic calculations [18] and experimental data [14, 15, 19, 58, 59].

	This work E_F	*Ab initio* calculations E_F	Atomistic simulations E_F	Experimental E_F
Li_2O	2.0	2.2 [33]		1.58–2.53 [19]
UO_2	4.1	3.9 [14]	5.4 [18]	4.6 ± 0.5 [58, 59]
				3.0–4.6 [14, 15]

available data [36–40] in figure 3 for both the systems. In Li_2O, the comparison is very good up to 1100 K beyond which the fast ion behaviour sets in and the slope of the experimental data [39] is much greater compared to that for the calculations [4]. We have incorporated the anharmonic corrections from the implicit effects involving volume thermal expansion in the quasiharmonic lattice dynamics calculations. For temperatures above $T = 1100$ K, in Li_2O explicit anharmonic effects involving contributions from higher order terms of the crystal potential become important; this gives rise to the disagreement between the lattice dynamics calculations and the reported data.

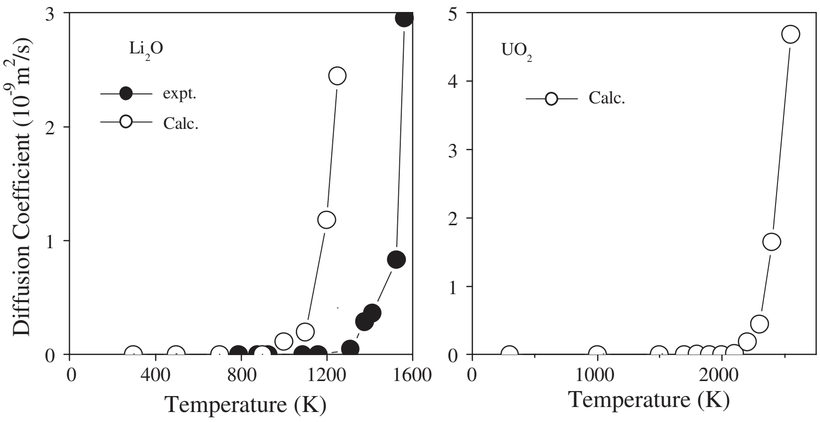

Figure 4. Diffusion coefficient of Li in Li_2O and O in UO_2, as a function of temperature. Open circles are the calculated values while closed circles are the experimental [57] values as taken from the literature.

Using 96-atom supercells, we have estimated the Frenkel defect energies (E_F), defined as the energy required for the formation of a vacancy/interstitial atom pair. While in Li_2O, it involves cation (Li) vacancy/interstitial pair formation, it involves the anions (O) in UO_2. Our calculated E_F values (table 2) are in satisfactory agreement with reported first-principles calculations [14, 33] and experimental data [15, 19]. As reported by various workers [16, 17, 36], defects are not believed to contribute significantly to the observed specific heat $C_P(T)$ of UO_2 and Li_2O in the 0–1600 K temperature range reported in the present study. In the case of UO_2 [36], in addition to the disordering of the oxygen sublattice, there are various other factors like electronic excitations, valence–conduction band transitions, etc which play a significant role in the anomalous increase in the specific heat which sets in above $T = 1600$ K [16], well before the fast ion transition. Hence the disagreement between computed and experimental specific heats is greater in the case of UO_2 as can be seen in figure 3.

3.3. Molecular dynamics results

The diffusion coefficient of the two oxides have been calculated from 300 to 1500 K in the case of Li_2O, and up to 3000 K in the case of UO_2 using molecular dynamics simulations (figure 4). The diffusion coefficient of Li [4] has been compared with available experimental data. The diffusion coefficient is comparable to that of a liquid in the superionic phase. Both the oxides show fast ion conduction as expected. Our molecular dynamics results suggest that the superionic phase sets in around 1000 K in the case of Li_2O while in UO_2 it sets in around 2300 K. Superionic conductivity is a complex phenomenon and the computed transition temperature ($T = 1000$ K) of Li_2O can be regarded as being in good agreement with the observed fast ion transition temperature of around 1200 K [57]. The signature of a corresponding superionic transition is found indirectly in the enthalpy studies on UO_2, since direct measurements are made difficult with high temperatures involved. It is found to undergo a Bredig transition (involving a jump in specific heat across the normal to superionic phase transition) at about 2610 K [16, 17]. To the best of our knowledge, there are no available experimental studies on the diffusion coefficient of oxygen ions in UO_2.

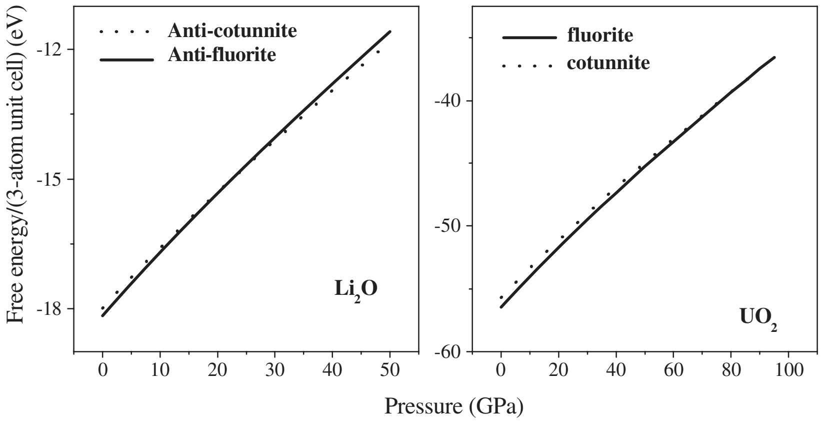

Figure 5. Calculated free energies of Li_2O (UO_2) which reveal anti-fluorite to anti-cotunnite (fluorite to cotunnite) phase transitions at pressures of 25 (70) GPa.

3.4. Phase transformations

These oxides are found to undergo pressure induced transformations to orthorhombic structures. Anti-fluorite lithium oxide undergoes a transition to the anti-cotunnite phase at pressures of about 50 GPa [41, 42]; this transition is accompanied by a relatively large volume collapse of ~5.4% and a large hysteresis upon pressure reversal, while the decreasing transition value of the pressure is found to be about 25 GPa.

Figure 5 gives the calculated free energies of the two phases with increasing pressure which reveal a free energy crossover and an anti-fluorite to anti-cotunnite phase transition at about 25 GPa for Li_2O. The ratio of the volume of the anti-cotunnite phase at this pressure with respect to the corresponding volume of the anti-fluorite at the same pressure is about 6%. In the case of UO_2, reported experimental studies [44, 45] reveal a sluggish transformation, wherein the cotunnite phase first appears at about 40 GPa and the fluorite phase is found to coexist even at 69 GPa. Our calculations (figure 5) show the transition point to be 70 GPa, with a volume decrease of about 3.5% with respect to the fluorite volume. This behaviour is in accordance to the structural variation of other superionic compounds with pressure.

4. Conclusions

Lattice dynamics calculations of the vibrational and thermodynamic properties of Li_2O and UO_2 have been carried out using shell models. The elastic constants, bulk modulus, equilibrium lattice constant and phonon frequencies are in very good agreement with reported data. Both the oxides show a transition to the fast ion phase at elevated temperatures. MD simulations reveal that Li_2O becomes superionic at around 1000 K while UO_2 shows a transition at around 2300 K. Diffusion coefficients at temperatures $T \sim 0.8T_m$ are comparable to those of liquids. As reported in the literature [41, 42], Li_2O shows a transition to an anti-cotunnite phase at around 25 GPa. UO_2 undergoes similar transformation at a higher pressure of 70 GPa.

References

[1] Hull S 2006 *Rep. Prog. Phys.* **67** 1233
[2] Farley T W D, Hayes W, Hull S, Hutchings M T J and Vrtis M 1991 *J. Phys.: Condens. Matter* **3** 4761
[3] Wyckoff R W G 1965 *Crystal Structures* 2nd edn (New York: Wiley)

[4] Goel P, Choudhury N and Chaplot S L 2004 *Phys. Rev.* B **70** 174307
[5] Carbajo J J, Yodu G L, Popuv S G and Ivanov V K 2001 *J. Nucl. Mater.* **299** 181
[6] van der Laan J G, Kawamura H, Roux N and Yamaki D 2000 *J. Nucl. Mater.* **283–287** 99
[7] Ralph J and Hyland G J 1985 *J. Nucl. Mater.* **132** 76
[8] MacInnes D A and Catlow C R A 1980 *J. Nucl. Mater.* **89** 354
[9] Manara D, Ronchi C, Sheindin M and Konings R 2007 *J. Nucl. Mater.* **362** 14
[10] Keen D A 2002 *J. Phys.: Condens. Matter* **14** R819
[11] Lindan P J D and Gillan M J 1994 *Phil. Mag.* B **69** 535
[12] Ruelloa P, Chirlesan G, Petit-Ervas G, Petit C and Desgranges L 2004 *J. Nucl. Mater.* **325** 202
[13] Hadari Z, Kroupp M and Wolfson M 1971 *J. Appl. Phys.* **42** 534
[14] Crocombette J P, Jollet F, Thien Nga L and Petit T 2001 *Phys. Rev.* B **64** 104107
[15] Matzke Hj 1987 *J. Chem. Soc., Faraday Trans.* 2 **83** 1121
[16] Ronchi C and Hyland G J 1994 *J. Alloys Compounds* **213/214** 159
[17] Ronchi C, Sheindlin M, Musella M and Hyland G J 1999 *J. Appl. Phys.* **85** 776
[18] Walker J R and Catlow C R A 1981 *J. Phys. C: Solid State Phys.* **14** L979
[19] Chadwick A V, Flack K W and Strange J H 1988 *Solid State Ion.* **28–30** 185
[20] Kalucinki G L 1986 *J. Nucl. Mater.* **141** 3
[21] Shah R, De Vita A, Heine H and Payne M C 1996 *Phys. Rev.* B **53** 8257
[22] Radeja J G 2001 *Modell. Simul. Mater. Eng.* **9** 81
[23] Fracchia R M, Barrera G D, Allan N, Baron T H K and Mackrodt W C 1998 *J. Phys. Chem. Solids* **59** 435
[24] Hull S and Keen D A 1998 *Phys. Rev.* B **58** 14387
[25] Keen D A and Hull S 1995 *J. Phys.: Condens. Matter* **7** 5793
[26] Hofmann M, Hull S, McIntyre G J and Wilson C C 1997 *J. Phys.: Condens. Matter* **9** 845
[27] Yashima M, Xu Q, Yoshiasa A and Wada S 2006 *J. Mater. Chem.* **16** 4393
[28] Kleppmann W G 1986 *J. Phys. C: Solid State Phys.* **19** 7167
[29] Elcombe M M and Pryor A W 1970 *J. Phys. C: Solid State Phys.* **3** 492
[30] Dickens M H, Hayes W, Schnabel P, Hutchings M T, Lechnu R E and Renker B 1983 *J. Phys. C: Solid State Phys.* **16** L1
[31] Hutchings M T, Clausen K, Dickens M H, Hayes W, Kjems J K, Schnabel P G and Smith C 1984 *J. Phys. C: Solid State Phys.* **12** 3941
[32] Wilkening M, Indus S and Hutjans P 2003 *Phys. Chem. Chem. Phys.* **5** 2225
[33] De vita A, Gilan M J, Lin J S, Payne M C, Srichand I and Clarke L J 1992 *Phys. Rev. Lett.* **68** 3319
[34] Browning P, Hyland G and Ralph J 1983 *High Temp.—High Pressures* **15** 169
[35] Clausen K, Hayes W, Hutchings M T, Kjems J K, Macdonald J E and Osborn R 1985 *High Temp. Sci.* **19** 189
[36] Fink J K, Chasanov M G and Leibowitz L 1981 *J. Nucl. Mater.* **102** 17
[37] Hyland G J and Ralph J 1983 *High Temp.–High Pressures* **15** 179
[38] Browning P 1981 *J. Nucl. Mater.* **98** 345
[39] Hull S, Farley T W D, Hayes W and Hutchings M T 1988 *J. Nucl. Mater.* **160** 25
[40] Tanifugi T, Shiozawa K and Nasu S 1978 *J. Nucl. Mater.* **78** 422
[41] Lazicki A, Yoo C S, Evans W J and Pickett P E 2006 *Phys. Rev.* B **73** 184120
[42] Kunc K, Loa I, Grechnik A and Syassen K 2005 *Phys. Status Solidi* b **242** 1857
[43] Cancarevic Z, Schon J C and Jaisu H 2006 *Phys. Rev.* B **73** 224114
[44] Idiri M, Le Bihan T, Heathman S and Rebizant J 2004 *Phys. Rev.* B **70** 014113
[45] Geng H Y, Chen Y, Kanita Y and Kinoshita M 2007 *Phys. Rev.* B **75** 054111
[46] Venkatraman G, Feldkamp L and Sahni V C 1975 *Dynamics of Perfect Crystals* (Cambridge, MA: MIT Press)
[47] Bruesh P 1986 *Phonons: Theory and Experiments* (Berlin: Springer)
[48] Rao K R, Chaplot S L, Choudhury N, Ghose S, Hastings J M, Corliss L M and Price D L 1988 *Phys. Chem. Minerals* **16** 83
[49] Chaplot S L, Choudhury N, Ghose S, Rao M N, Mittal R and Goel P 2002 *Eur. J. Minerology* **14** 291
[50] Chaplot S L 1978 *Report* BARC-972
[51] Chaplot S L 1992, unpublished
[52] Chaplot S L and Rao K R 1987 *Phys. Rev.* B **35** 9771
[53] Chaplot S L 1990 *Phys. Rev.* B **42** 2149
[54] Chaplot S L and Choudhury N 2001 *Am. Mineral.* **86** 752
[55] Farley T W D, Hayes W, Hull S and Ward R 1988 *Solid State Ion.* **28–30** 189
[56] Dolling C, Cowley R and Woods A D B 1965 *Can. J. Phys.* **43** 1397
[57] Oishi Y, Kamwei Y and Akuryama M 1979 *J. Nucl. Mater.* **87** 341
[58] Clausen K, Hayes W, Macdonald J E, Osborn R and Hutchings M T 1984 *Phys. Rev. Lett.* **52** 1238
[59] Hutchings M T 1987 *J. Chem. Soc. Faraday Trans.* 2 **83** 1083–103